AIP Journal of Applied Physics

Influence of spin relaxation length on lateral double superconductor/ferromagnet/superconductor junctions

L. K. Lin, S. Y. Huang, J. K. Lin, J. H. Huang, and S. F. Lee

Citation: Journal of Applied Physics **109**, 07E155 (2011); doi: 10.1063/1.3565411
View online: http://dx.doi.org/10.1063/1.3565411
View Table of Contents: http://scitation.aip.org/content/aip/journal/jap/109/7?ver=pdfcov
Published by the AIP Publishing

Influence of spin relaxation length on lateral double superconductor/ferromagnet/superconductor junctions

L. K. Lin,[1,2] S. Y. Huang,[1] J. K. Lin,[1] J. H. Huang,[2] and S. F. Lee[1,a)]
[1]*Institute of Physics, Academia Sinica, Taipei 115, Taiwan, Republic of China*
[2]*Department of Materials Science and Engineering, National Tsing Hua University, HsinChu 300, Taiwan, Republic of China*

(Presented 16 November 2010; received 21 September 2010; accepted 1 January 2011; published online 8 April 2011)

We study the spin dependent transport at the junctions between two superconducting Nb leads connected by two ferromagnetic NiFe bars in parallel, which have various separations. The separation distance l between NiFe bars was varied from 150 to 700 nm to study the spin relaxation effect in Nb. In small l (150 and 250 nm) samples, a spin-valve-like behavior related to the inverse proximity effect was observed, which manifest itself as charge accumulation due to spin imbalance near the interface. However, for samples with large l, the spin-valve behavior vanishes and the anisotropic magnetoresistance effect dominates. © *2011 American Institute of Physics*. [doi:10.1063/1.3565411]

I. INTRODUCTION

Electron transport in ferromagnet (F) and conventional s wave superconductor (S) hybrid structures exhibits several remarkable phenomena. The S prefers an antiparallel spin orientation in the Cooper pairs, while the F favors the spins to align in parallel by exchange force. The singlet wavefunction of the Cooper pairs from the S can penetrate a short distance into the F, which is one example of the proximity effect.[1–4] Recently, focus was put on the inverse proximity effect.[5–7] The ferromagnetic order-parameter can also penetrate into the S and induce net magnetization near the interface. In this case, a possible triplet pairing is induced in the S-F structures. The spin switch characterization, which shows a resistance difference when the relative orientations are parallel (P) and antiparallel (AP) between the two F magnetizations, is found in recent investigations of S-F spin-valve multilayered thin films due to proximity effect.[8–10] Similar behavior is also observed in the lateral S-F system[11] and is explained by the spin accumulation in terms of inverse proximity effect rather than the crossed Andreev reflection (CAR) or elastic co-tunneling (EC).[12,13] In Ref. 11, the physical origin of the spin switch behavior was attributed to the nonzero subgap electronic density of state in a region extending in the S by means of inverse proximity effect. In this region, the spins from one F can travel through a long distance and cross talk to the other F. In this report, we study the influence of the spin relaxation on the spin switch effect in a S-F lateral hybrid system with larger range of separation between two Fs.[14–16]

The scanning electron microscope images of our sample geometries are shown in Fig. 1. In each sample, two Nb pads are connected through two NiFe bars in parallel. The two bars were made with different dimensions (1 μm $\times$ 300 nm and 2 μm $\times$ 600 nm) to obtain different coercive fields. The average switching fields of the small and large bars are 125 and 235 Oe, respectively, with variations between samples due to the lithography process. However, the difference of the switching fields in each sample can be clearly observed. We have chosen a pointed end shape of the bar in order to obtain a single magnetic domain within one bar. The separation distance l between two NiFe bars is varied from 150 to 700 nm shown as Fig. 1(a) to 1(d). Figure 1(e) shows the schematic drawing of the sample geometry. The gap between two Nb pads is about 250 nm, which is much larger than the proximity effect decay length in a F metal. Samples are prepared by electron beam lithography and lift-off technique. The thickness of 30 nm NiFe bars and 3 nm Au protecting layer are deposited by dc magnetron sputtering onto Si substrates coated with SiO_2 in the first step. After the second electron beam lithography, 80 nm Nb is deposited covering two NiFe bars to ensure the superconducting behavior of Nb pads. Prior to the deposition of Nb, the protecting layer is removed by a soft ion milling. The transport properties were measured with magnetic fields parallel to the two NiFe bars under various temperatures.

Figure 2 shows the resistance versus temperature dependence of the $l = 250$ nm sample at low temperature and from 2 to 300 K in the inset. A linear dependence of resistance from 50 to 300 K represents a metallic transport behavior. The resistance from the residue resistance 36.8 Ω drops to 35.5 Ω around $T_c = 8.3$ K indicating the superconducting behavior occurs in the Nb pads. Because the Nb pads are connected through the two NiFe bars, the resistance drops to a certain nonzero value contributed from the two bars.

The two NiFe bars with different dimensions show clearly different magnetization switching fields, which is observed in separately made array samples by magneto-optical Kerr effect (MOKE) measurements. We have measured the electron transport properties of a series of samples at low temperature under the T_c of the Nb pads. Both magnetizations of the two NiFe bars were first saturated with a magnetic field of 3000 Oe. The field was then swept down to -3000 Oe and the resistance

a)Electronic mail: leesf@phys.sinica.edu.tw.

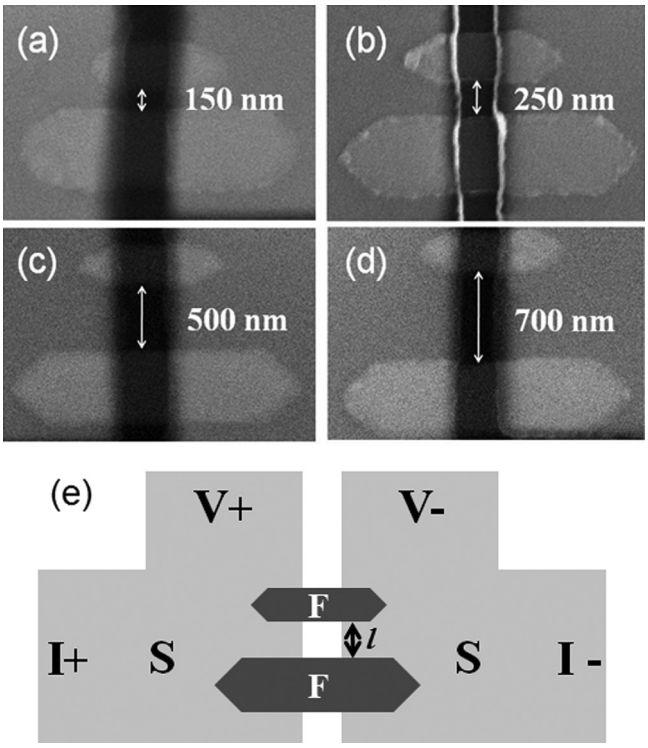

FIG. 1. Scanning electron microscope images of the samples with two superconducting Nb pads covering two ferromagnetic NiFe bars in parallel, which have various separated distance as in (a) 150, (b) 250, (c) 500, and (d) 700 nm. (e) A schematic drawing shows the sample geometry.

was measured. This procedure was repeated from -3000 Oe sweeping up to 3000 Oe. In this way, we systematically measured the resistance of each samples in different magnetization configurations. The magnetoresistance (MR) measurement on the $l = 150$ nm sample is shown in Fig. 3(a). Several different resistance states are observed. The low and high resistance states represent the *AP* and *P* magnetization configurations. Some meta-stable states with intermediate resistance on the MR curve are observed. The switching fields of the NiFe bars are different from the average values, especially the small bar.

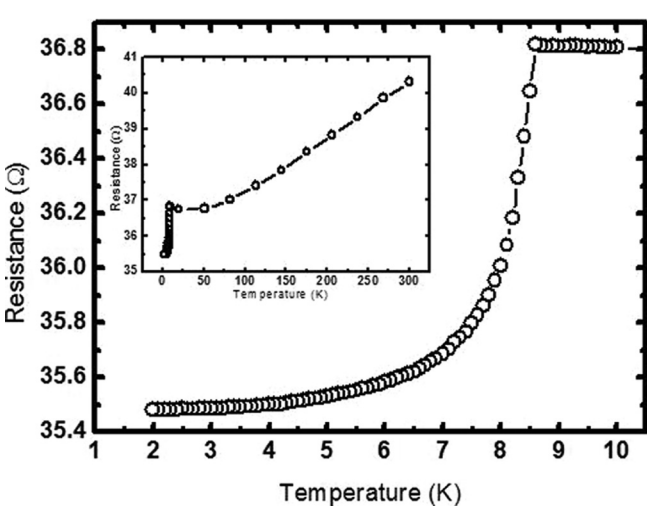

FIG. 2. Resistance vs temperature dependence from 2 to 10 K of the 250 nm separation sample, showing a transition temperature of 8.3 K. (inset) Resistance versus temperature curve from 2 to 300 K.

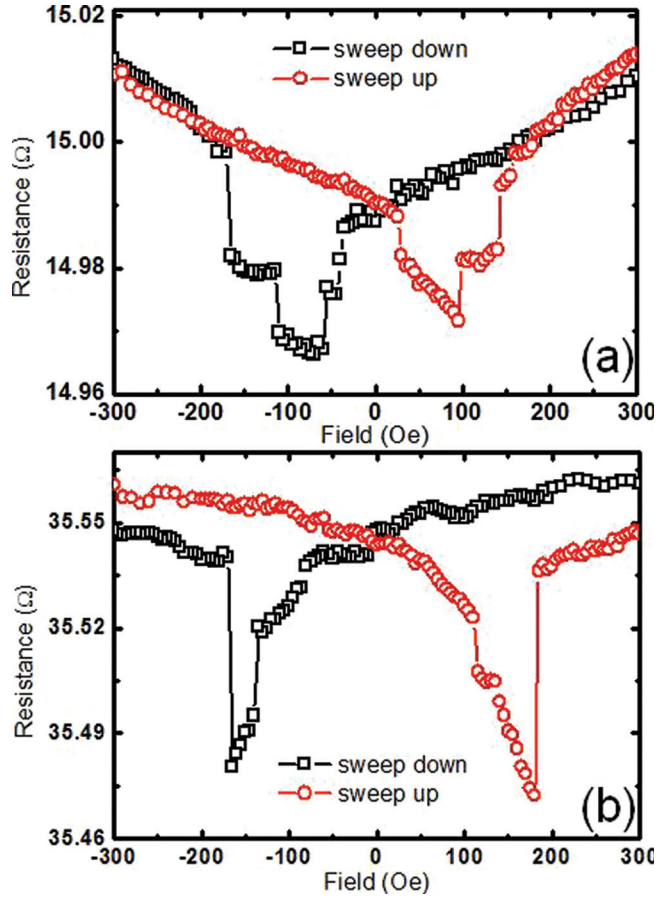

FIG. 3. (Color online) Magnetoresistance curves of (a) the 150 nm separation sample measured at 7.4 K, below the superconducting transition temperature, and (b) the 250 nm separation sample measured at 2 K.

It could be attributed to the magnetization multi-domain reversal process due to the defects and/or impurities of the NiFe bars. In Fig. 3(b), the spin-valve behavior is also clearly observed in the $l = 250$ nm sample exhibiting different switching fields. The resistance differences between the *P* and *AP* states are about 0.2% in both small l (150 and 250 nm) samples. The MR measurements at 2 K on the large l (500 and 700 nm) samples are shown in Fig. 4. There are four unambiguous dips in the curves and the MR ratios are 0.05% and 0.07% of $l = 500$ and 700 nm samples. The magnitude of MR ratio is distinct to the spin-valve effect. We ascribe the behavior to a combination of the anisotropic magnetoresistance (AMR) effect independently taking place in the two NiFe bars. The inner and outer dips are respectively caused by the small and large bar and are corresponding to the switching fields of AMR. The separation distance between two bars is too large to couple the spin information and form the spin-valve states. It could be regarded as an independent AMR effect measurement of two *F* bars in parallel measured by the same superconducting electrodes. At *S*-*F* junction, a spin-polarized current is converted into a spinless current when electrons go from *F* into *S*. There is inverse proximity effect taking place at a region in *S* near the $S-F$ interface of Nb pads. In *P* state, the current through both bars injects the same majority spins. When the separation distance of two bars is shorter than a characteristic length scale in Nb, a spin accumulation builds up at the $S-F$

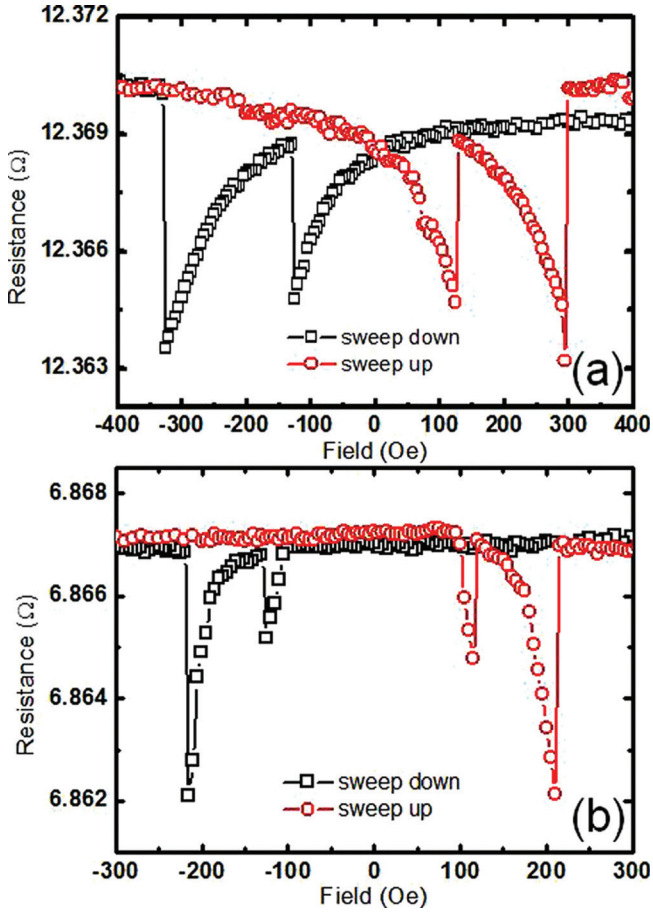

FIG. 4. (Color online) Magnetoresistance curves measured at 2 K of (a) the 500 nm separation sample, and (b) the 700 nm separation sample.

interfaces. In *AP* state, one bar injects more spin-up quasiparticles and the other one injects more spin-down quasiparticles. The two spin populations are balanced and less spin accumulation is expected. Thus, the *AP* state is expected to have a lower voltage drop than the *P* state, as measured in the small l (150 and 250 nm) samples. As discussed in Ref. 11, the region in the Nb pads surrounding the two *F* bars should be governed by the spin relaxation length λ_{sf}. In the small separation distance, spin information could be transferred from one magnetic bar to the other, and spin-valve behavior reveals. The spin accumulation effect is expected to dissipate at large distance. When the inverse proximity effect occurs, the region near the $S-F$ interface extends over a few times of the superconducting coherence length ξ_S in S,[5] which is estimated to be 12 nm.[17] The l should be compared to the characteristic length scale, the spin relaxation length λ_{sf} in Nb. All coherent correlations are expected to be lost beyond λ_{sf}. The electron spin relaxation length can be described by $\lambda_{sf}=(D\tau_{sf})^{1/2}$ where the D is diffusion coefficient and τ_{sf} is spin relaxation time. There are two different way could be found in the literature to determine the λ_{sf}. In current-perpendicular-to-plane (CPP) spin-valve structures, the λ_{sf} in Nb is estimated to be 25 and 48 nm by transport measurements.[18,19] The other way to estimate the λ_{sf} is the nonlocal measurements by lateral spin diffusion.[14–16] In the lateral dimension, the spins can travel through several hundred nanometers.[20] In our results, the dual AMR effect is observed rather than the spin-valve effect in the large l samples. It is consistent with the lateral spin diffusion experiments that the spin relaxation length λ_{sf} is in the range from 250 to 500 nm in Nb.

In summary, we investigate the spin dependent transport at the junction between two Nb leads covering two ferromagnetic NiFe bars in parallel. A significant spin-valve behavior was observed in the samples with small l (150 and 250 nm). This spin-valve behavior is related to the inverse proximity effect in terms of spin accumulation due to spin imbalance near the interface. The spin-valve behavior vanished and the anisotropic magnetoresistance effect dominated in the samples with large l (500 and 700 nm). Thus, spin relaxation length λ_{sf} in Nb is ensured in the range between 250 and 500 nm in lateral dimension.

The financial supports of Academia Sinica and the National Science Council of Taiwan, Republic of China are gratefully acknowledged.

[1]E. A. Demler, G. B. Arnold, and M. R. Beasley, Phys. Rev. B **55**, 15174 (1997).
[2]L. Lazar, K. Westerholt, H. Zabel, L. R. Tagirov, Yu. V. Goryunov, N. N. Garif'yanov, and I. A. Garifullin, Phys. Rev. B **61**, 3711 (2000).
[3]A. I. Buzdin, Rev. Mod. Phys. **77**, 935 (2005).
[4]S. Y. Huang, Y. C. Chiu, J. J. Liang, L. K. Lin, T. C. Tsai, S. Y. Hsu, and S. F. Lee, J. Appl. Phys. **105**, 07E319 (2009).
[5]M. A. Sillanpää, T. T. Heikkilä, R. K. Lindell, and P. J. Hakonen, Europhys. Lett. **56**, 590 (2001).
[6]M. Yu. Kharitonov, A. F. Volkov, and K. B. Efetov, Phys. Rev. B **73**, 054511 (2006).
[7]Jing Xia, V. Shelukhin, M. Karpovski, A. Kapitulnik, and A. Palevski, Phys. Rev. Lett. **102**, 087004 (2009).
[8]J. Y. Gu, C.-Y. You, J. S. Jiang, J. Pearson, ya. B. Bazaliy, and S. D. Bader, Phys. Rev. Lett. **89**, 267001 (2002).
[9]A. Yu. Rusanov, S. Habraken, and J. Aarts, Phys. Rev. B **73**, 060505 (2006).
[10]R. Steiner and Ziemann, Phys. Rev. B **74**, 094504 (2006).
[11]P. S. Luo, T. Crozes, B. Gilles, S. Rajauria, B. Pannetier, and H. Courtois, Phys. Rev. B **79**, 140508 (2009).
[12]Guy Deutscher and Denis Feinberg, Appl. Phys. Lett. **76**, 487 (2000).
[13]P. Cadden-Zimansky and V. Chandrasekhar, Phys. Rev. Lett. **97**, 237003 (2006).
[14]F. J. Jedema, B. J. van Wees, B. H. Hoving, A. T. Filip, and T. M. Klapwijk, Phys. Rev. B **60**, 16549 (1999).
[15]S. Takahashi and S. Maekawa, J. Phys. Soc. Jpn. **77**, 031009 (2008).
[16]N. Poli, J. P. Morten, M. Urech, Arne Brataas, D. B. Haviland, and V. Korenivski, Phys. Rev. Lett. **100**, 136601 (2008).
[17]S. Y. Huang, S. F. Lee, S. Y. Hsu, and Y. D. Yao, Phys. Rev. B **76**, 024521 (2007).
[18]Wanjun Park, David V. Baxter, S. Steenwyk, I. Moraru, W. P. Pratt, Jr., and J. Bass, Phys. Rev. B **62**, 1178 (2000).
[19]J. Y. Gu, J. A. Caballero, R. D. Slater, R. Loloee, and W. P. Pratt, Jr., Phys. Rev. B **66**, 140507 (2002).
[20]J. Bass and W. P. Pratt, Jr., J. Phys.: Condens. Matter **19**, 183201 (2007).